

Machine-Learning-based Prediction of Lattice Thermal Conductivity for Half-Heusler Compounds using Atomic Information

Hidetoshi Miyazaki^{1*}, Tomoyuki Tamura^{1, 2}, Masashi Mikami³, Kosuke Watanabe¹, Ide Naoki¹, Osman Murat Ozkendir⁴, and Yoichi Nishino¹

¹ *Nagoya Institute of Technology, Dept. of Physical Science and Engineering, 466-8555, Nagoya, Japan*

² *Center for Materials research by Information Integration, National Institute for Materials Science (NIMS), Tsukuba 305-0047, Japan*

³ *National Institute of Advanced Industrial Science and Technology, 2266-98 Anagahora, Shimoshidami, Moriyama, Nagoya 463-8560*

⁴ *Tarsus University, Institute of Natural Science, Dept. of Nanotechnology and Advanced Materials, 33400, Tarsus, Turkey*

Keywords: Half-Heusler compounds; machine learning; thermal conductivity.

*miyazaki@nitech.ac.jp

ABSTRACT

The half-Heusler compound has drawn attention in a variety of fields as a candidate material for thermoelectric energy conversion and spintronics technology. This is because it has various electronic structures, such as semi-metals, semiconductors, and a topological insulator. When the half-Heusler compound is incorporated into the device, the control of high lattice thermal conductivity owing to high crystal symmetry is a challenge for the thermal manager of the device. The calculation for the prediction of lattice thermal conductivity, which is an important physical parameter for controlling the thermal management of the device, requires a calculation cost of several 100 times as much as the usual density functional theory calculation. Therefore, we examined whether lattice thermal conductivity prediction by machine learning was possible on the basis of only the atomic information of constituent elements for thermal conductivity calculated by the density functional theory calculation in various half-Heusler compounds. Consequently, we constructed a machine learning model, which can predict the lattice thermal conductivity with high accuracy from the information of only atomic radius and atomic mass of each site in the half-Heusler type crystal structure. Applying our results, the lattice thermal conductivity for an unknown half-Heusler compound can be immediately predicted. In the future, low-cost and short-time development of new functional materials can be realized, leading to breakthroughs in the search of novel functional materials.

I. INTRODUCTION

Thermal conductivity is a physical quantity representing how heat is transferred from one side of a

material to the other when thermal energy is applied. It is one of the most fundamental and important physical quantities. Moreover, it is an important physical quantity in terms of application, which is necessary for the understanding of thermal management to ensure the performance, life-time, and safety for thermoelectric energy conversion devices, and spintronics technology.

Thermal conductivity can be divided into electron and lattice contributions. The thermal conductivity of electrons can be determined from the electrical conductivity using the Wiedemann-Franz law. Half-Heusler compounds show high lattice thermal conductivities due to their high degrees of crystal symmetry. Therefore, it is necessary to know the exact lattice thermal conductivity for thermal management in half-Heusler devices. Theoretical predictions of the lattice thermal conductivity of solids can be made using nonequilibrium molecular dynamics simulations [1–7] or the density functional theory (DFT) calculations [8–16]. The prediction of thermal conductivity by nonequilibrium molecular dynamics requires an enormous amount of computational time because time evolution must be calculated for numerous atomic movements. However, because DFT can accurately calculate interactions between atoms, thermal conductivity can be predicted several hundred times. Presently, theoretical studies of the lattice thermal conductivity are limited to systems with a small number of atoms in the unit cell, such as simple pure metals [8, 11, 16], binary materials [9, 13–17], and full and half-Heusler compounds [12, 18–21]. Therefore, it is difficult to perform comprehensive lattice thermal conductivity calculations for a large number of materials.

Cubic half-Heusler compounds have drawn significant attention in various fields as candidate materials for thermoelectric energy conversion [22–27] and spintronics technology [28–32]. This is because it has various electronic structures, such as semi-metals, semiconductors, and a topological insulator. Jesus Carrete *et al.* [33] and Jianghui Liu *et al.* [34] attempted to predict the lattice thermal conductivity of half-Heusler compounds obtained from the results of the DFT calculations by machine learning (ML). Jesus Carrete *et al.* reported that the lattice thermal conductivity of half-Heusler compounds can be predicted in the range of 10% using the Young's modulus value obtained from the DFT calculations as the descriptor for the ML. Jianghui Liu *et al.* reported that the lattice thermal conductivity of half-Heusler compounds can be predicted in the range of 10% using the atomic numbers, atomic masses, and atomic radii of the constituent atoms of half-Heusler compounds as the descriptors for ML.

The prediction of the lattice thermal conductivity must be highly accurate to predict the performance of thermoelectric materials and thermal management of electronic devices. Therefore, we have developed a ML algorithm to predict the lattice parameter and lattice thermal conductivity of half-Heusler compounds from the atomic information of their constituent atoms (atomic radius and atomic mass) only. This algorithm can predict lattice thermal conductivity values with high accuracy of less than 4% for many half-Heusler compounds. In this study, we found that the lattice thermal conductivity of the half-Heusler compounds, which is difficult to predict using the DFT calculations, can be predicted with

high accuracy by ML. This report will provide a breakthrough in the development of new materials, as it can contribute to the discovery of innovative materials for next-generation thermoelectric conversion and spintronics materials, and other technologies requiring thermal management in the future.

II. CALCULATION METHODS

Evaluation of site selection of the half-Heusler structure and lattice parameter

Candidate half-Heusler compounds for lattice thermal conductivity calculations were sought from the Materials Project [35]. In the crystal structure of $C1_b$ -type half-Heusler compounds, there are three types of atomic sites: $4a$ (0, 0, 0), $4b$ (0.5, 0, 0), and $4c$ (0.25, 0.25, 0.25) sites. The $4a$ and $4b$ sites are crystallographically interchangeable. Three structural models can be considered as one of the three constituent elements occupies the $4c$ site and the other two elements occupy the $4a$ and $4b$ sites. The lattice parameters were optimized using the DFT calculations for the three models. By comparing the total energies of the three models, the structural model with the lowest energy was determined to be the most stable structural model for the half-Heusler compound. The DFT calculations were performed using the Vienna *ab initio* Simulation Package (VASP) [36–38]. We adopted the projector augmented-wave (PAW) method [39, 40] with the generalized gradient approximation of Perdew, Burke, and Ernzerhof [41] for the exchange–correlation interactions.

Evaluation of lattice thermal conductivity of half-Heusler compounds

The lattice thermal conductivity of half-Heusler compounds was calculated using the Phono3py code, developed by Atushi Togo *et al* [17], for various positions of atoms in a supercell made of $2 \times 2 \times 2$ primitive cells. Although the lattice thermal conductivity shows a temperature dependence, herein, we discuss the lattice thermal conductivity at 300 K. The calculated lattice thermal conductivities and lattice parameters are summarized in Table S1 in the Supplementary materials section.

Machine Learning of thermal conductivity of half-Heusler compounds

Figure 1 shows a flowchart of the ML used to predict the lattice parameter and lattice thermal conductivity in half-Heusler compounds. The atomic radii, r_1 , r_2 , r_3 , and atomic masses, m_1 , m_2 , m_3 , of the elements at $4c$, $4a$, and $4b$ sites in the $C1_b$ -type crystal structure were used as descriptors. The Python library Pymatgen, Python Materials Genomics [42], was used to obtain the elemental information. The swapped data set of the elemental information of the $4a$ and $4b$ sites was also created because the $4a$ and $4b$ sites are interchangeable. First, to build an ML model to predict the lattice parameters, the atomic radii and masses were used as descriptors. Second, to build a ML model to predict the calculated lattice thermal conductivity, the parameters generated by various combinations of atomic masses, atomic radii, and the lattice parameters were used. The parameters of the combinations of atomic radii and atomic masses used for lattice thermal conductivity prediction are listed in Table S2 in the Supplementary materials section. Finally, to find the best combination of parameters, we used the Wrapper method with a backward feature elimination to sequentially remove unimportant parameters hence build an optimal

ML model for predicting the lattice thermal conductivity. For lattice parameter and lattice thermal conductivity prediction, the multiple linear regression and boosted decision tree regression models were used as the ML models. The hyperparameters were adjusted by random sweeps to adjust the optimal hyperparameters. Python 3.6 was used for implementing the ML model. The training and test data were split between 80% and 20%. We used 5-fold cross validation on the data set to evaluate the decision coefficients using the test data for each fold, and the mean of the decision coefficients, R^2 , was used to evaluate the ML model.

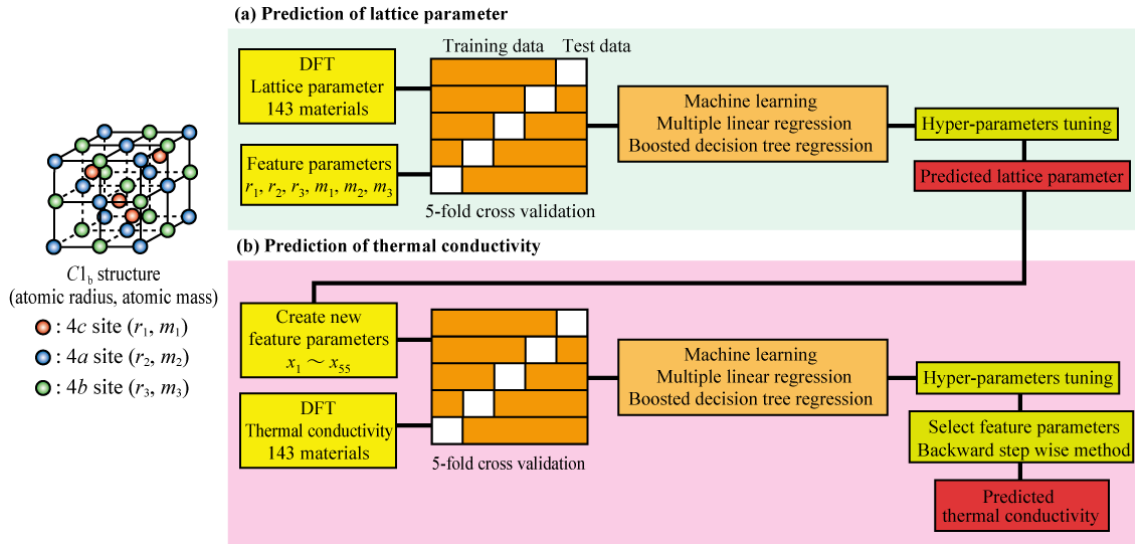


FIG. 1

Flowchart of the ML used to predict (a) lattice parameter and (b) thermal conductivity.

III. RESULTS and DISCUSSIONS

Figures 2 (a1), (a2), and (a3) show the results of ML using multiple linear regression of the lattice parameters for various half-Heusler compounds obtained from the structural optimization by DFT calculations. ML with multiple linear regression predicts the lattice parameter with a higher accuracy using the atomic masses and atomic radii than that using the atomic radii only. As described in Table S.1, the stability of half-Heusler compounds is affected by the atomic radii of each site and the atomic masses. Therefore, besides the atomic radii, the atomic masses have an important influence on the lattice parameter determination. The prediction of the lattice parameter using multiple linear regression can be determined with an accuracy of approximately 5%, as shown in Figure 2 (a3). To determine the lattice parameter with a better accuracy, we performed ML by boosted decision tree regression as shown in Figures 2 (b1), (b2), and (b3). Using the atomic radius and mass as parameters, R^2 improved to 0.979. As shown in Fig. 1 (b3), the ML model reproduced the lattice parameter almost perfectly with an accuracy of approximately $\pm 1\%$. The boosted decision tree regression using the atomic radii and masses

of the atoms at the three sites of the $C1_b$ -type structure as a description was found to be the most suitable for predicting the lattice parameter by ML.

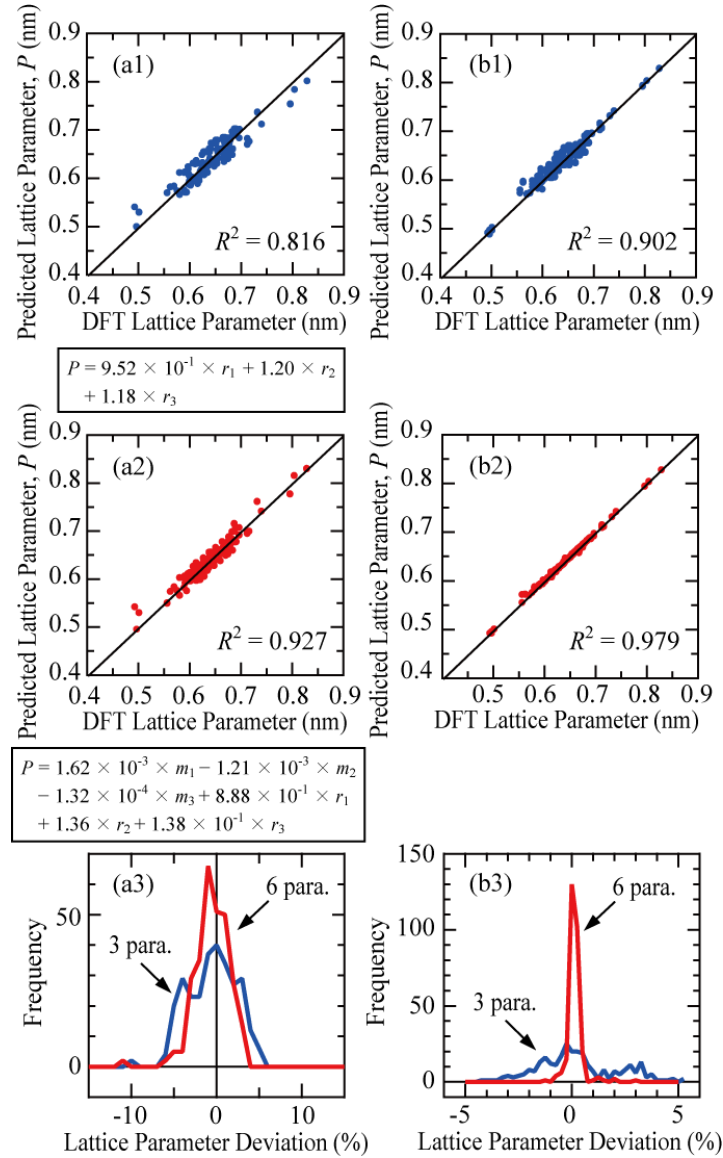


FIG. 2

Comparison between the lattice parameters predicted by the ML model of multiple linear regression (a1, a2, a3) and boosted decision tree regression (b1, b2, b3) and the lattice parameters calculated by the DFT calculation. (a1, b1) and (a2, a3) are the results of ML using a combination of atomic radii (3 parameters) and atomic mass and atomic radius (6 parameters) as descriptors, respectively. The regression equations determined by multiple linear regression are shown at the bottom of figures (a1, a2). (a3, b3) Frequency of deviations between the calculated and predicted lattice parameters.

Figures 3 show the results of the predicted lattice thermal conductivity for various half-Heusler

compounds using ML with multiple linear regression and boosted decision tree regression. As shown in Figure 3(a), the boosted decision tree regression model shows a higher coefficient of determination than the multiple linear regression model, and reproduces the thermal conductivity of the half-Heusler compounds well. The ML model, such as a simple multiple linear regression is not suitable for ML of the lattice thermal conductivities. This result suggests that the lattice thermal conductivity exhibits a high accuracy owing to the complex interaction of various descriptors. Figure 3(b) shows the feature importance scores for the 55 parameters in ML of boosted decision tree regression. Among the 55 parameters, the top 4 parameters make a significant contribution to the accuracy of ML. It is known that when many 55 parameters are used in ML, the prediction accuracy is reduced because of over-fitting. It is necessary to find the best combination of parameters to improve the prediction accuracy of the lattice thermal conductivity. Figure 3(c) shows the results of the evaluation by the Wrapper Method using backward feature elimination. The backward feature elimination calculates the permutation feature importance of each parameter and sequentially removes the unimportant parameter to find the optimal combination of parameters. The R^2 for the ML of thermal conductivity using the top four parameters is the highest R^2 of 0.84, which is an improvement over the R^2 when all the parameters are considered. The best parameter combination of the important features score for the prediction of the lattice thermal conductivity are in the following order:

(Top 1) x_{55} : lattice parameter.

(Top 2) x_{42} : the difference between the mean atomic radius of the constituent elements and the atomic radius of the 4c site, $(r_1 + r_2 + r_3) / 3 - r_1$.

(Top 3) x_{33} : the difference between the mean atomic mass of the constituent elements and the atomic mass of the 4c site, $(m_1 + m_2 + m_3) / 3 - m_1$.

(Top 4) x_{29} : the sum of the atomic masses, $m_1 + m_2 + m_3$.

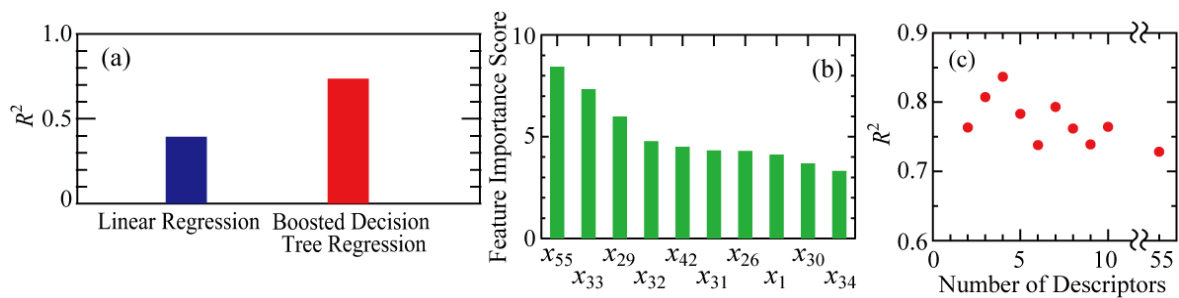


FIG. 3.

(a) R^2 for the ML model of multiple linear regression and boosted decision tree regression performed on the calculated lattice thermal conductivity. (b) Top 10 parameters of permutation feature importance for each parameter in the ML model of boosted decision tree regression. (c) Dependence of the number of features on the R^2 evaluated by the wrapper Method with backward feature elimination.

Figures 4(a1) and 4(a2) show the results of lattice thermal conductivity predicted by ML for the boosted decision tree regression described with 55 and 4 parameters, respectively. The predictions of thermal conductivity with 4 parameters are in a better agreement with the results of ML with 55 parameters. Figure 4(b) shows the number of deviations between the predicted and calculated lattice thermal conductivities by the ML model of the boosted decision tree regression with 55 and 4 parameters. When 55 parameters were used, the lattice thermal conductivity was overestimated, with a deviation of approximately 8%. Conversely, when 4 parameters were used to describe the lattice thermal conductivity, the accuracy improved to approximately $\pm 4\%$. Jesus Carrete *et al* [33] and Jianghui Liu *et al* [34] have previously reported that the accuracy of the lattice thermal conductivity prediction in half-Heusler compounds predicted by ML is approximately $\pm 10\%$. In this study, our ML model using the lattice parameter as a descriptor and selecting an appropriate combination of atomic radii and atomic masses as a descriptor led to a significant improvement in the accuracy of the prediction of lattice thermal conductivity.

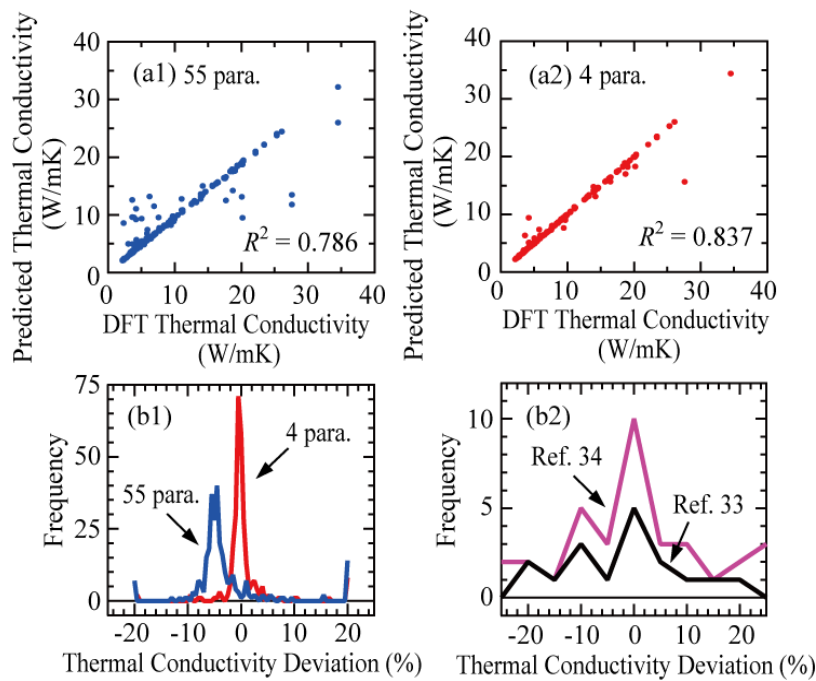


FIG. 4

(a1, a2) Comparison between the lattice thermal conductivity predicted by the ML model of boosted decision tree regression using 55, and 4 parameters and the lattice thermal conductivity calculated by the DFT calculation. (b1) Number of deviations between the predicted and calculated lattice thermal conductivity using 55 and 4 parameters. (b2) Number of deviations between the predicted and calculated lattice thermal conductivity reported by Jesus Carrete *et al* [33] and Jianghui Liu *et al* [34].

Figure 5 plots the relationship between three parameters and thermal conductivity, which are important

in determining the lattice thermal conductivity of half-Heusler compounds. For many compounds with large lattice parameters, the lattice thermal conductivity is below 6, which is a low lattice thermal conductivity material. The lattice thermal conductivity of a solid material is expressed by the equation $\kappa \sim C v l$, where C , v , and l represent the specific heat, sound velocity, and phonon mean free path, respectively. It is essential to reduce the thermal conductivity to improve the performance of thermoelectric conversion materials. For this purpose, C , v , and l should be reduced. However, it is difficult to change C and l significantly in the same crystal system. The lattice thermal conductivity is lower in a compound with a large sum of atomic mass, including the structure and small lattice parameter because the sound velocity is expressed as a function inversely proportional to the density. Therefore, for compounds with small lattice parameters, the decrease in thermal conductivity can be qualitatively explained by the decrease in sound velocity. In half-Heusler compounds with lattice parameters of 0.7 to 0.8, the thermal conductivity is below 4 for the systems BaNaSb, KBaSb, CaCdSn, and KSrSb with large differences between the average atomic mass and $4c$ sites in the compounds. Even in half-Heusler compounds with large lattice parameters, small lattice thermal conductivities can be achieved by selecting the heavy elements to occupy the $4c$ site.

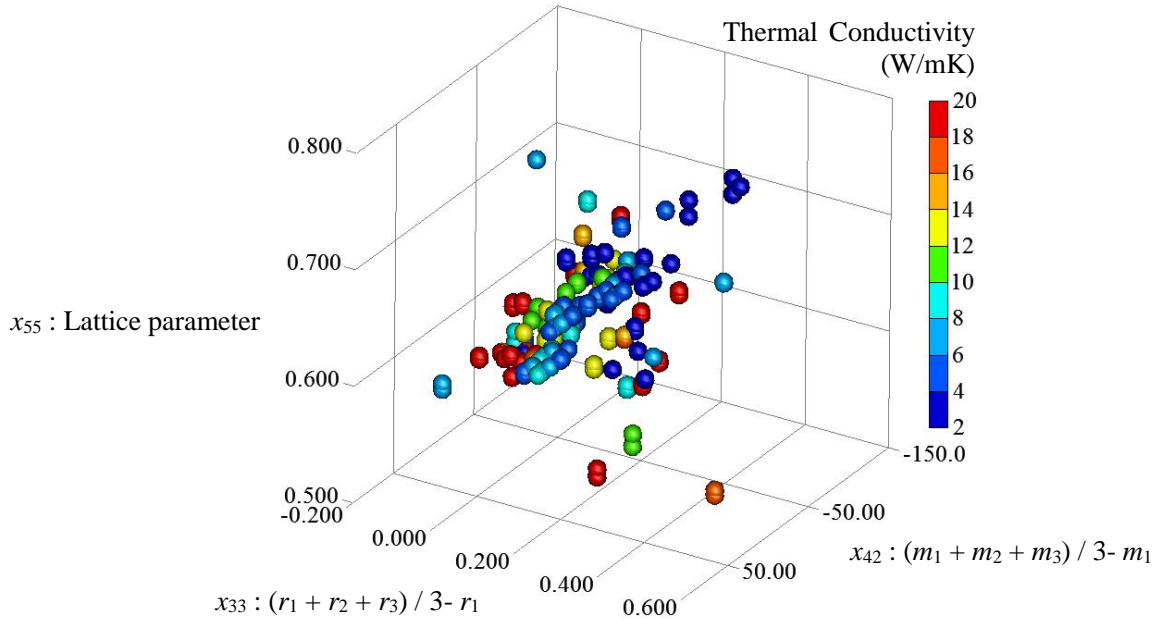


FIG. 5.

3D plots of the three parameters (x_{33} , x_{42} , x_{55}) and predicted lattice thermal conductivity. The magnitude of the lattice thermal conductivity in 3D plotting is shown in color scale.

The material design of half-Heusler compounds has focused on compounds with elements from groups 1 to 4 applied to the $4a$ site, elements from groups 12 to 16 applied to the $4b$ site, and elements from

groups 8 to 11 applied to the $4c$ site. This study revealed that many half-Heusler compounds contain groups 14 to 16 elements at the $4c$ site and groups 1 and 2 elements at the $4a$ and $4b$ sites. When heavier elements, such as Sn and Sb, occupy the $4c$ site, the difference between the average atomic weights is particularly large, and such compounds are predicted to show considerably decreased thermal conductivities. In the future, the synthesis of these groups of materials will lead to new low thermal conductivity half-Heusler compounds.

IV. Conclusion

In this study, we investigated whether the lattice thermal conductivity of half-Heusler compounds can be predicted by ML from the atomic radii and masses of the constituent elements. The results show that the lattice thermal conductivity of the half-Heusler compounds can be predicted with an accuracy of $\pm 4\%$ using the predicted lattice parameters and the atomic radii and masses. In addition to the conventional material design in which a material with a small lattice parameter and low density has a low thermal conductivity, it was found that even for materials with a large lattice parameter, one can design a material with a low thermal conductivity by selecting elements occupying the $4c$ site of the half-Heusler structure with a larger atomic mass than those occupying the $4a$ and $4b$ sites. Using the results of ML, the thermal conductivity of unknown half-Heusler compounds can be instantly predicted. It is expected that the search for half-Heusler compounds with the desired thermal conductivity will become easier and the development of functional materials in a short time and at a low cost will be advanced in the future.

SUPPLEMENTARY MATERIALS

See supplementary materials for the periodic table of the site selection system of the 143 half-Heusler compounds and the complete results of the calculated lattice parameter and thermal conductivity and list of parameters for ML used for thermal conductivity prediction

ACKNOWLEDGEMENTS

The computations were performed by the Research Center for Computational Science, Okazaki, Japan. This study was partly supported by the Japan Society for the Promotion of Science's (JSPS) Grants-in-Aid for Scientific Research (KAKENHI) (C) (17K06771, 18K04700, 18K04748, 20K05100, and 20K05060). We would like to thank Editage (www.editage.com) for English language editing.

REFERENCES

- [1] Florian Müller-Plathe, J. Chem. Phys. 106, 6082 (1997).
- [2] Sebastian G. Volz, Appl. Phys. Lett. 75, 2056 (1999).
- [3] Sebastian G. Volz and Gang Chen, Phys. Rev. B 61, 2651 (2000).
- [4] J. E. Turney, E. S. Landry, A. J. H. McGaughey, and C. H. Amon, Phys. Rev. B 79, 064301 (2009).
- [5] E. Lampina, P. L. Palla, P.-A. Francioso, and F. Cleri, J. Appl. Phys. 114, 033525 (2013).

- [6] K. Tanaka, S. Ogata, R. Kobayashi, T. Tamura, and T. Kouno, *Int. J. Heat Mass Transf.* 89, 714 (2015).
- [7] Mohamed S. El-Genk, Khaled Talaat, and Benjamin J. Cowen, *J. Appl. Phys.* 123, 205104 (2018).
- [8] D. A. Broido, M. Malorny, G. Birner, N. Mingo, and D. A. Stewart, *Appl. Phys. Lett.* 91, 231922 (2007).
- [9] A. Ward and D. A. Broido, *Phys. Rev. B* 77, 245328 (2008).
- [10] A. Ward and D. A. Broido, *Phys. Rev. B* 81, 085205 (2010).
- [11] K. Esfarjani, G. Chen, and H. T. Stokes, *Phys. Rev. B* 84, 085204 (2011).
- [12] J. Shiomi, K. Esfarjani, and G. Chen, *Phys. Rev. B* 84, 104302 (2011).
- [13] Z. Tian, J. Garg, K. Esfarjani, T. Shiga, J. Shiomi, and G. Chen, *Phys. Rev. B* 85, 184303 (2012).
- [14] T. Shiga, J. Shiomi, J. Ma, O. Delaire, T. Radzynski, A. Lusakowski, K. Esfarjani, and G. Chen, *Phys. Rev. B* 85, 155203 (2012).
- [15] L. Lindsay, D. A. Broido, and T. L. Reinecke, *Phys. Rev. Lett.* 109, 095901 (2012).
- [16] L. Chaput, *Phys. Rev. Lett.* 110, 265506 (2013).
- [17] A. Togo, L. Chaput, and I. Tanaka, *Phys. Rev. B*, 91, 094306 (2015).
- [18] G. Ding, G. Y. Gao, and K. L. Yao, *J. Phys. D: Appl. Phys.* 48 235302 (2015).
- [19] P. Hermet and P. Jund, *J. Alloys Compd.* 668, 248 (2016).
- [20] S. N. H. Eliassen, A. Katre, G. K. H. Madsen, C. Persson, O. M. Løvvik, and K. Berland, *Phys. Rev. B* 95, 045202 (2017).
- [21] S. H. Han, Z. Z. Zhou, C. Y. Sheng, J. H. Liu, L. Wang, H. M. Yuan, and H. J. Liu, *J. Phys.: Condens. Matter*, 32 425704 (2020).
- [22] Y. Kawaharada, H. Uneda, H. Muta, K. Kurosaki, and S. Yamanaka, *J. Alloys Compd.* 364, 59 (2004).
- [23] S. Sakurada and N. Shutoh, *Appl. Phys. Lett.* 86, 082105 (2005).
- [24] T. Zhu, C. Fu, H. Xie, Y. Liu and X. Zhao, *Adv. Energy Mater.* 5, 1500588 (2015).
- [25] E. Rausch, B. Balke, J. M. Stahlhofen, S. Ouardi, U. Burkhardt, and C. Felser, *J. Mater. Chem. C* 3, 10409-10414 (2015).
- [26] Y. Chai, T. Oniki, T. Kenjo, Y. Kimura, *J. Alloys Compd.* 662, 566 (2016).
- [27] Y. Tang, X. Li, L. H. J. Martin, E. C. Reyes, T. Ivas, C. Leinenbach, S. Anand, M. Peters, G. J. Snyder, and C. Battaglia, *Energy Environ. Sci.* 11, 311 (2018).
- [28] R. A. de Groot, F. M. Mueller, P. G. van Engen, and K. H. J. Buschow, *Phys. Rev. Lett.* 50, 2024 (1983).
- [29] L. Feng, E. K. Liu, W. X. Zhang, W. H. Wang, and G. H. Wu, *J. Magn. Magn. Mater.* 351, 92 (2014).
- [30] R. L. Zhang, L. Damewood, Y. J. Zeng, H. Z. Xing, C. Y. Fong, L. H. Yang, R. W. Peng, and C. Felser, *J. Appl. Phys.* 122, 013901 (2017).
- [31] J. Ma, V. I. Hegde, K. Munira, Y. Xie, S. Keshavarz, D. T. Mildebrath, C. Wolverton, *Phys. Rev. B* 95, 024411 (2017).
- [32] A. Dehghan and S. Davatolhagh, *J. Alloys Compd.* 772, 132 (2019).

- [33]J. Carrete, Wu Li, N. Mingo, S. Wang, and S. Curtarolo, *Phys. Rev. X* 4, 011019 (2014).
- [34]J. Liu, S. Han, G. Cao, Z. Zhou, C. Sheng and H. Liu, *J. Phys. D: Appl. Phys.* 53, 315301 (2020).
- [35]A. Jain, S.P. Ong, G. Hautier, W. Chen, W.D. Richards, S. Dacek, S. Cholia, D. Gunter, D. Skinner, G. Ceder, K.A. Persson, *APL Materials* 1, 011002 (2013).
- [36]G. Kresse and J. Hafner, *Phys. Rev. B* 48, 13115 (1993).
- [37]G. Kresse and J. Furthmuller, *Comput. Mater. Sci.* 6, 15 (1996).
- [38]G. Kresse and J. Furthmuller, *Phys. Rev. B* 54, 11169 (1996).
- [39]P. E. Blochl, *Phys. Rev. B* 50, 17953 (1994).
- [40]G. Kresse and D. Joubert, *Phys. Rev. B* 59, 1758 (1999).
- [41]J. P. Perdew, K. Burke, and M. Ernzerhof, *Phys. Rev. Lett.* 77, 3865 (1996).
- [42] S. P. Ong, W. D. Richards, A. Jain, G. Hautier, M. Kocher, S. Cholia, D. Gunter, V. L. Chevrier, K. Persson, G. Ceder, *Comput. Mater.* 68, 314 (2013).

SUPPLEMENTARY MATERIALS

Figure S1 shows the periodic table of the site selection system of the constituent elements for the 143 half-Heusler compounds. The elements from groups 8 to 11 occupy almost $4c$ sites; groups 1 to 6 and the lanthanide and actinide series occupy $4a$ sites and some elements also occupy $4b$ sites. The elements of groups 12–16 occupy $4b$ sites as well as $4c$ sites for most of the elements. This suggests that the site selection in half-Heusler compounds is not determined solely by the relationship between the atomic radii of the elements at each site but also by the atomic masses at each site, which is a complex balance of the two elemental information.

Site Selection Legend:

- Red: $4c$ site
- Blue: $4a$ site
- Green: $4b$ site

Crystal Structure: $C1_b$ structure

	1	2	3	4	5	6	7	8	9	10	11	12	13	14	15	16	17	18
1	H																	He
2	Li	Be											B	C	N	O	F	Ne
3	Na	Mg											Al	Si	P	S	Cl	Ar
4	K	Ca	Sc	Ti	V	Cr	Mn	Fe	Co	Ni	Cu	Zn	Ga	Ge	As	Se	Br	Kr
5	Rb	Sr	Y	Zr	Nb	Mo	Tc	Ru	Rh	Pd	Ag	Cd	In	Sn	Sb	Te	I	Xe
6	Cs	Ba	L	Hf	Ta	W	Re	Os	Ir	Pt	Au	Hg	Tl	Pb	Bi	Po	At	Rn
7	Fr	Ra	A	Rf	Db	Sg	Bh	Hs	Mt	Ds	Rg	Cn	Nh	Fl	Mc	Lv	Ts	Og
	L	57 La	58 Ce	59 Pr	60 Nd	61 Pm	62 Sm	63 Eu	64 Gd	65 Tb	66 Dy	67 Ho	68 Er	69 Tm	70 Yb	71 Lu		
	A	89 Ac	90 Th	91 Pa	92 U	93 Np	94 Pu	95 Am	96 Cm	97 Bk	98 Cf	99 Es	100 Fm	101 Md	102 No	103 Lr		

FIG. S1

Periodic table summarizing the site-selective system for each element in the half-Heusler compound determined by DFT calculations.

TABLE S1

Table of the Materials ID, Chemical formula, optimal site locations, lattice parameters, and thermal conductivities for 143 half-Heusler compounds. The atoms occupying each site and the corresponding lattice parameter are shown for the optimal site selection with the lowest total energy. Thermal conductivities are calculated using the lattice thermal conductivity calculation code Phonopy3 for the best site combination.

Materials ID	Chemical Formula	4c site	4a site	4b site	L. P.	T. C.
2894	ScSnAu	Au	Sc	Sn	0.653	7.09
3161	LiAlSi	Si	Li	Al	0.594	5.90
3432	ScNiSb	Ni	Sc	Sb	0.612	13.91
3462	TmSnAu	Au	Tm	Sn	0.669	4.61
3522	MgCuSb	Cu	Mg	Sb	0.625	3.68
3716	TbNiSb	Ni	Tb	Sb	0.639	9.06
4025	TmNiSb	Ni	Tm	Sb	0.631	9.85
4174	HoNiSb	Ni	Ho	Sb	0.635	9.69
4262	BeAlB	B	Be	Al	0.496	18.71
4510	DyNiSb	Ni	Dy	Sb	0.636	9.46
4964	YSbPt	Pt	Y	Sb	0.663	3.23
5177	LuSnAu	Au	Lu	Sn	0.666	4.72
5640	ErSnAu	Au	Er	Sn	0.671	4.53
5920	LiAlGe	Ge	Li	Al	0.601	5.08
5967	TiCoSb	Co	Ti	Sb	0.590	22.13
7173	ScSbPt	Pt	Sc	Sb	0.640	7.67
7575	LiZnN	N	Li	Zn	0.493	17.39
9124	LiZnAs	As	Li	Zn	0.598	13.89
9437	NbFeSb	Fe	Nb	Sb	0.596	23.43
10194	LuSbPt	Pt	Lu	Sb	0.655	6.42
10687	LiCdP	P	Li	Cd	0.614	20.07
11242	DyPbAu	Au	Dy	Pb	0.685	3.35
11520	YNiSb	Ni	Y	Sb	0.638	9.03
11836	ErSbPd	Pd	Er	Sb	0.657	7.65
11839	GdSbPt	Pt	Gd	Sb	0.666	3.34
11869	HfSnPd	Pd	Hf	Sn	0.637	13.99
12558	LiMgAs	As	Li	Mg	0.620	20.18
13308	HoGeAu	Au	Ho	Ge	0.653	4.34
16313	TbSbPt	Pt	Tb	Sb	0.664	3.82
16314	TmSbPt	Pt	Tm	Sb	0.657	5.86
16327	DySbPt	Pt	Dy	Sb	0.662	4.43
16329	ErSbPt	Pt	Er	Sb	0.659	5.41
16376	HoSbPt	Pt	Ho	Sb	0.661	4.95
19886	ThSnPt	Pt	Th	Sn	0.683	4.15
20185	LuNiSb	Ni	Lu	Sb	0.628	9.97
20269	MnGaPt	Pt	Mn	Ga	0.600	2.33
20415	GdPbAu	Au	Gd	Pb	0.689	3.18
20514	GdSnAu	Au	Gd	Sn	0.679	3.73
20952	TiNiSb	Ni	Ti	Sb	0.596	3.64
21272	ErNiSb	Ni	Er	Sb	0.633	9.68
21425	UNiSn	Ni	U	Sn	0.636	5.36
22786	ThNiSn	Ni	Th	Sn	0.660	7.15
30377	ErPbAu	Au	Er	Pb	0.682	3.51
30389	HoPbAu	Au	Ho	Pb	0.684	3.43
30390	HoSnAu	Au	Ho	Sn	0.673	4.46
30413	TbPbAu	Au	Tb	Pb	0.687	3.26
30453	DyBiPt	Pt	Dy	Bi	0.675	6.23
30454	ErBiPt	Pt	Er	Bi	0.672	6.35
30455	HoBiPt	Pt	Ho	Bi	0.674	6.46
30457	LuNiBi	Ni	Lu	Bi	0.641	9.83
30459	ScNiBi	Ni	Sc	Bi	0.627	9.06
30460	YNiBi	Ni	Y	Bi	0.651	5.91
30847	TiSnPt	Pt	Ti	Sn	0.624	11.18
30848	USnPt	Pt	U	Sn	0.667	5.41
31451	ZrCoBi	Co	Zr	Bi	0.624	17.68
31454	TaSbRu	Ru	Ta	Sb	0.620	16.23
31455	VSbRu	Ru	V	Sb	0.605	6.90
31457	ZrSbRu	Ru	Zr	Sb	0.636	3.36
36111	LiMgP	P	Li	Mg	0.600	19.94
505297	NbSbRu	Ru	Nb	Sb	0.620	15.65
567418	HoSbPd	Pd	Ho	Sb	0.659	7.72
567422	GdNiBi	Ni	Gd	Bi	0.653	8.12
567636	VFeSb	Fe	V	Sb	0.580	14.20
568269	TmNiBi	Ni	Tm	Bi	0.644	9.36
569197	GdNiSb	Ni	Gd	Sb	0.641	8.38
569779	ScSbPd	Pd	Sc	Sb	0.639	11.07
570213	LiMgBi	Bi	Li	Mg	0.682	15.77
620271	GdBiPt	Pt	Gd	Bi	0.679	5.54
621592	YPbAu	Au	Y	Pb	0.687	3.28
924128	HfNiSn	Ni	Hf	Sn	0.612	16.44

924129	ZrNiSn	Ni	Zr	Sn	0.616	19.05
924130	TiNiSn	Ni	Ti	Sn	0.596	17.54
961646	TiTeOs	Os	Ti	Te	0.618	12.96
961649	ZrFeTe	Fe	Zr	Te	0.610	20.00
961653	FeSiW	Fe	Si	W	0.556	6.21
961657	YNiP	Ni	Y	P	0.598	2.37
961659	TiSiPd	Pd	Ti	Si	0.589	25.31
961660	TiFeSe	Fe	Ti	Se	0.562	27.60
961661	ZrSiPd	Pd	Zr	Si	0.612	18.35
961665	MgScGa	Ga	Mg	Sc	0.647	3.88
961673	TiFeTe	Fe	Ti	Te	0.589	20.30
961675	ScNiP	Ni	Sc	P	0.569	8.87
961678	ScCoTe	Co	Sc	Te	0.607	12.70
961682	TiSnPd	Pd	Ti	Sn	0.622	11.03
961684	LiCaAs	As	Li	Ca	0.667	20.16
961685	NaCaAs	As	Na	Ca	0.696	7.57
961687	ZrSnPd	Pd	Zr	Sn	0.641	14.04
961693	ZrInAu	Au	Zr	In	0.653	9.42
961697	ScGeAu	Au	Sc	Ge	0.630	12.52
961698	LiZnP	P	Li	Zn	0.576	9.72
961706	TiSiPt	Pt	Ti	Si	0.591	34.51
961711	ZrSiPt	Pt	Zr	Si	0.615	14.11
961713	ZrSnPt	Pt	Zr	Sn	0.643	13.23
961774	BaNaSb	Sb	Ba	Na	0.796	2.17
962063	LaMgTl	Tl	La	Mg	0.731	6.26
962068	CaMgSn	Sn	Ca	Mg	0.716	4.19
962069	LiAgTe	Te	Li	Ag	0.664	3.38
962078	CaCdSi	Si	Ca	Cd	0.670	3.39
1008624	YBiPd	Pd	Y	Bi	0.674	4.24
1008680	TiGePt	Pt	Ti	Ge	0.600	19.40
1008858	NdBiPd	Pd	Nd	Bi	0.687	4.59
1009006	LiCdAs	As	Li	Cd	0.634	16.44
1009132	HoBiPd	Pd	Ho	Bi	0.672	6.78
1009543	DyBiPd	Pd	Dy	Bi	0.673	6.93
1018118	TmSbPd	Pd	Tm	Sb	0.656	7.66
1018135	LiCdAs	As	Li	Cd	0.634	16.49
1018139	HoNiBi	Ni	Ho	Bi	0.647	9.44

1076916	GdBiPd	Pd	Gd	Bi	0.677	6.80
1093991	ZrAsIr	Ir	Zr	As	0.618	10.43
1094088	NbCoSn	Co	Nb	Sn	0.597	18.62
1100391	NaBeSb	Be	Na	Sb	0.625	3.62
1100392	LiSiB	B	Li	Si	0.501	11.09
1100393	LiAgSe	Se	Li	Ag	0.628	2.72
1100403	KBaSb	Sb	K	Ba	0.828	2.88
1100404	VAsRu	Ru	V	As	0.580	5.04
1100409	LiCaSb	Sb	Li	Ca	0.712	26.07
1100411	CaCdSn	Sn	Ca	Cd	0.712	3.02
1100412	TiTeRu	Ru	Ti	Te	0.615	14.54
1100420	NaCaSb	Sb	Na	Ca	0.740	5.45
1100424	LiMgSb	Sb	Li	Mg	0.667	14.63
1100425	LiCdSb	Sb	Li	Cd	0.674	3.51
1100429	KSrSb	Sb	K	Sr	0.804	3.66
1100430	LiZnSb	Zn	Li	Sb	0.632	4.81
1100433	CaZnSi	Si	Ca	Zn	0.648	2.46
1100436	LiInSi	Si	Li	In	0.628	3.61
1206667	PrNiBi	Ni	Pr	Bi	0.668	4.47
1206679	YBiPt	Pt	Y	Bi	0.676	4.61
1206681	ScBiPd	Pd	Sc	Bi	0.653	5.85
1206686	TbNiBi	Ni	Tb	Bi	0.651	8.57
1206712	ErNiBi	Ni	Er	Bi	0.646	9.68
1206717	LaBiPd	Pd	La	Bi	0.696	4.35
1206719	NdNiBi	Ni	Nd	Bi	0.665	5.25
1206720	PrBiPd	Pd	Pr	Bi	0.690	4.19
1206744	TmBiPd	Pd	Tm	Bi	0.669	6.28
1206953	ErBiPd	Pd	Er	Bi	0.670	6.53
1206989	TbBiPt	Pt	Tb	Bi	0.677	5.90
1206992	LuBiPt	Pt	Lu	Bi	0.668	5.77
1207057	TmBiPt	Pt	Tm	Bi	0.670	5.94
1207082	LiMgSb	Sb	Li	Mg	0.667	14.63
1207177	TbBiPd	Pd	Tb	Bi	0.675	6.93
1207185	LuBiPd	Pd	Lu	Bi	0.666	5.75
1216635	TiSnIr	Ir	Ti	Sn	0.622	3.90
1225491	DySbPd	Pd	Dy	Sb	0.661	7.67

TABLE S2

List of parameters for machine learning used for thermal conductivity prediction. It is listed by various combinations of atomic mass (m_1, m_2, m_3) and atomic radius (r_1, r_2, r_3) of elementals at $4c, 4a, 4b$ site. The lattice parameter, x_{55} , uses the predicted values of the lattice parameters obtained by the multiple linear regression in Fig. 2(b2).

	Parameters		Parameters		Parameters
x_1	m_1	x_{20}	$\sqrt{m_2}$	x_{39}	x_{33}^2
x_2	m_2	x_{21}	$\sqrt{m_3}$	x_{40}	x_{34}^2
x_3	m_3	x_{22}	$\sqrt{r_1}$	x_{41}	x_{35}^2
x_4	r_1	x_{23}	$\sqrt{r_2}$	x_{42}	$x_{30}/3 - r_1$
x_5	r_2	x_{24}	$\sqrt{r_3}$	x_{43}	$x_{30}/3 - r_2$
x_6	r_3	x_{25}	m_2/m_1	x_{44}	$x_{30}/3 - r_3$
x_7	m_1^2	x_{26}	r_3/m_1	x_{45}	$ x_{42} $
x_8	m_2^2	x_{27}	r_2/r_1	x_{46}	$ x_{43} $
x_9	m_3^2	x_{28}	r_3/r_1	x_{47}	$ x_{44} $
x_{10}	r_1^2	x_{29}	$m_1 + m_2 + m_3$	x_{48}	x_{42}^2
x_{11}	r_2^2	x_{30}	$r_1 + r_2 + r_3$	x_{49}	x_{43}^2
x_{12}	r_3^2	x_{31}	$((m_1^2 + m_2^2 + m_3^2)/3)^2$	x_{50}	x_{44}^2
x_{13}	m_1^3	x_{32}	$((r_1^2 + r_2^2 + r_3^2)/3)^2$	x_{51}	$r_1^2 + r_2^2$
x_{14}	m_2^3	x_{33}	$x_{29}/3 - m_1$	x_{52}	$r_1^2 + r_3^2$
x_{15}	m_3^3	x_{34}	$x_{29}/3 - m_2$	x_{53}	$\sqrt{x_{51}}$
x_{16}	r_1^3	x_{35}	$x_{29}/3 - m_3$	x_{54}	$\sqrt{x_{52}}$
x_{17}	r_2^3	x_{36}	$ x_{33} $	x_{55}	Predicted lattice parameter
x_{18}	r_3^3	x_{37}	$ x_{34} $		
x_{19}	$\sqrt{m_1}$	x_{38}	$ x_{35} $		